Understanding the mechanism of base-assisted decomposition of (*N*-halo),*N*-alkylalcoholamines.

J. Andrés,[a] X.L. Armesto,[b] M. Canle L.,[b] M.V. García,[b] D.R. Ramos† [b] and J.A. Santaballa*[b]

[a] *Departament de Ciències Experimentals. Universitat Jaume I. Campus de Riu Sec. E-12071 Castelló. Spain. Fax: +34 964 728066; Tel.: +34 964 728083; E-mail: andres@exp.uji.es.*
[b] *Departamento de Química Física e Enxeñería Química I. Universidade da Coruña. Rúa Alejandro de la Sota 1. E-15008 A Coruña. Spain. Fax: +34 981 167065; Tel.: +34 981 167000; E-mail: armesto@udc.es, mcanle@udc.es, vicky@udc.es, danielr@udc.es, arturo@udc.es.*

The base-assisted decomposition of (*N*-X),*N*-methylethanolamine (X = Cl, Br) takes place mainly through two concurrent processes: a fragmentation and an intramolecular elimination. The global process follows second order kinetics, first order relative to both (*N*-X),*N*-methylethanolamine and base. Interaction of the base with the ionizable hydroxylic hydrogen triggers the reaction. The intramolecular elimination pathway leads to formaldehyde and 2-amino ethanol as reaction products *via* base-assisted proton transfer from the methyl to the partially unprotonated hydroxylic oxygen, with loss of halide. Meanwhile, the fragmentation pathway leads to methylamine and two equivalents of formaldehyde *via* bimolecular base-promoted concerted breakage of the molecule into formaldehyde, halide ion and *N*-methylmethanimine. Kinetic evidences allow a crude estimation of the concertedness and characterization of the transition structure for both processes, which are slightly asynchronous, the proton transfer to the base taking place ahead of the rest of molecular events. The degree of asynchroneity increases as the bases become weaker. Electronic structure calculations, at the B3LYP/6-31++G** level, on the fragmentation pathway support the proposed mechanism.

Introduction.

Halogenation is of considerable relevance in the cell metabolism of mammalians.[1] Thus, enzymatic chlorination of amino derivatives, such as taurine, has proved to be essential in leucocyte protection against infection in mammalians,[2-4] and has also been related to cell lysis[4] and other disorders related to inflammation.[5] On the other hand, chlorination is still the most used method of water treatment,[6] with well documented benefits and drawbacks.[7] Relationships between water chlorination and cancer have been reported.[8]

Alcoholamines are widely used in industry,[9] and as a result occur in residual and wastewaters. Recent studies[10,11] explained the base-promoted decomposition of some secondary (*N*-X)-alcoholamines in terms of a cooperative four-pathway mechanism as depicted in Scheme 1, *i.e.*: Hoffmann and Zaitsev intermolecular eliminations,[12] a Grob fragmentation,[13] and an intramolecular elimination.[10] The main process was found to be intramolecular elimination for the HO^--promoted decomposition of (*N*-Cl),*N*-ethylethanolamine, and Grob fragmentation in the case of the HO^--promoted decomposition of (*N*-Cl),*N*-tertbutylethanolamine.[10]

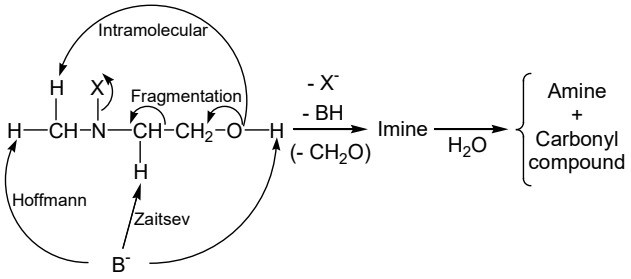

Scheme 1. Potential decomposition pathways for (*N*-X),*N*-alkylalcoholamines.

Here, we report a joint kinetic and theoretical study of the base-promoted decomposition of (*N*-X),*N*-methylethanolamine. The mechanism of the process differs from the one previously proposed[10] in the intramolecular elimination process being concerted and general-base catalysed and, more particularly, in that the proposed fragmentation step corresponds to an unprecedented concerted base-assisted fragmentation.

Experimental.

Chemicals and solutions.

N-Methylethylamine (Fluka, 95%) and *N*-methylethanolamine (Merck, >98%) were halogenated *in situ* using fresh HOCl and HOBr solutions, as described elsewhere,[10,14] to obtain 2 mM aqueous solutions of (*N*-X)-amines in all cases. Solutions of NaOH (Merck, *p.a.*), and buffers of 2,2,2-trifluoroethanol / 2,2,2-trifluoroethoxide (Aldrich, 99%+, pK_a=12.43),[15] and 1,1,1,3,3,3-hexafluoro-2-propanol / 1,1,1,3,3,3-hexafluoro-2-propoxide (Aldrich, 99%+, pK_a=9.30),[15] were used to control pH. Ionic strength was set to 1.0 M using NaCl or KCl (Merck, *p.a.*), the latter in the kinetic runs involving buffers. All other chemicals were of the highest purity available and used without further purification. Organic matter-free, twice-distilled water was used to make up all solutions.

Kinetic measurements.

Reactions were studied in all cases under pseudo-first order conditions, following the decrease of the UV bands of the (*N*-X)-amines (λ_{max} (*N*-Cl) = 265 nm, λ_{max} (*N*-Br) = 303 nm). A double-beam Varian® Cary 1E spectrophotometer and a Hi-Tech Scientific® SF-61 stopped-flow spectrophotometer were used. Samples were placed in Suprasil quartz cells and thermostated at 298.15 ± 0.1 K, unless otherwise indicated. pH measurements were carried out using a properly calibrated combined glass electrode.

Product analysis.

Product analyses of formaldehyde and amines, reported in Table 1, were carried out by HPLC with UV detection. All analyses were performed at least in duplicate and the results averaged. Quantitative determination of amines was made by derivatization to the corresponding phenylthioureas with phenyl isothiocyanate

Table 1. Amount of final reaction products found per mol of reacted (*N*-X),*N*-methylethanolamine in the presence of HO^-.

Product	(*N*-Cl)-compound	(*N*-Br)-compound
CH_3NH_2	0.67 ± 0.01	0.55 ± 0.02
$NH_2CH_2CH_2OH$	0.33 ± 0.01	0.45 ± 0.02
CH_2O	1.41 ± 0.05	1.80 ± 0.09

(Fluka, *puriss.* ≥99%) at 313 K and pH *ca*. 7 (50 mM phosphate buffer) during 30 min, then brought to completion at room temperature. The absorbance of the derivatised products was measured at 248 nm. The mobile phase used was CH_3CN/H_2O (50:50 v:v), flowing at 1 mL·min^{-1}, 20 µL of sample being injected in all cases. The linearity of response of the detector to all analysed products was checked. A reversed-phase 250 mm length, 4.6 mm internal diameter Sugelabor® column, packed with C-18 Inertsil ODS2, 5 µm, was used in an Agilent® 1100 series chromatograph. Using this method, the retention times found were: 3.27 min for ethanolamine, 3.76 min for *N*-methylethanolamine, 4.15 min for methylamine, 5.18 min for ethylamine and 5.86 min for *N*-methylethylamine.

Analysis of formaldehyde was also performed by derivatization with dinitrophenylhydrazine (Merck, *p.a.*).[16] A reversed-phase 250 mm length, 4.6 mm internal diameter Sugelabor® column, packed with C-18 Partisil ODS3, 5 µm, and protected with a 7.5 mm length, 4.6 mm internal diameter Sugelabor® precolumn, filled with the same stationary phase, were used in a Waters® 600s/717plus/996 chromatograph. The presence of reaction products other than aldehydes was proved to interfere under the study conditions, leading to deviations from the real formaldehyde concentrations.

Computational details.

All calculations have been performed using the Gaussian 98 suite of programs.[17] Density functional theory calculations were carried out by using the B3LYP/6-31++G** level.[18-20]

The model comprises a molecule of (*N*-Cl),*N*-methylethanolamine, a HO^- in the vicinity of the hydroxylic hydrogen and to roughly simulate the first solvation shell two water molecules were also included, one located close to the HO^- and the other close to the amino group. Geometry, energy, and frequencies of stationary points for the fragmentation pathway, *i.e.* isolated reactants (R), reactant interaction complex (RIC), transition structure (TS), product interaction complex (PIC), and isolated products (P), have been characterized. In all cases real frequencies were obtained, except for the transition structure where only one imaginary frequency was found. Wyberg bond indexes[21] have also been computed over the optimised structures by using the natural bond orbital (NBO) analysis as implemented in Gaussian 98.[17,22,23] To include the bulk effect of solvation single point calculations were carried out, over the *in vacuo* optimized structures, using the polarizable continuum model (PCM).[24]

Results and Discusion.

In alkaline media and at constant hydroxide ion concentration, the reaction follows a pseudo-first order rate dependence on the (*N*-X),*N*-methylethanolamine concentration:

$$r = k_{obs}\cdot[(N\text{-X}),N\text{-methylethanolamine}] \quad (1)$$

The observed rate constant, k_{obs}, is linearly dependent on $[HO^-]$, as shown in Figure 1.

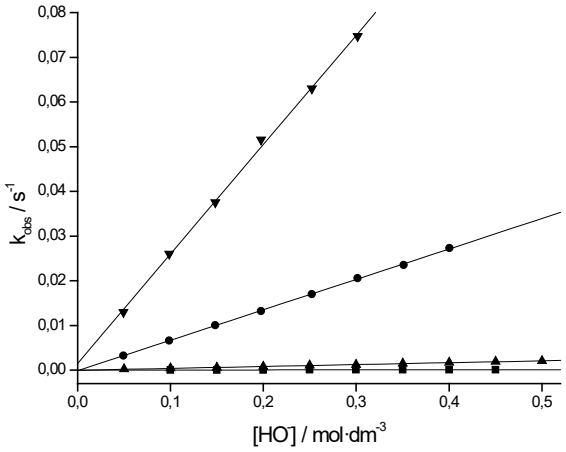

Figure 1. Dependence of k_{obs} vs $[HO^-]$. (●) (*N*-Cl),*N*-methylethanolamine, (■) (*N*-Cl),*N*-methylethylamine, (▼) (*N*-Br),*N*-methylethanolamine, (▲) (*N*-Br),*N*-methylethylamine. [(*N*-X)-amine]=2.00·10^{-3} mol·dm^{-3}, I = 1.0 mol·dm^{-3}, T = 298.15 K.

Linear dependences on base concentration are also observed when other bases are present *i.e.*:

$$k_{obs} = \Sigma\, k_B\cdot[B] \quad (2)$$

where k_B is the second order rate constant corresponding to each base present in the reaction media. The values of k_B are collected in Table 2.

(*N*-X)-alcoholamines decompose much faster than the corresponding parent (*N*-X)-amines in all cases. In accordance with this, k_{HO^-} for reaction of (*N*-X),*N*-methylethanolamine with HO^- is two orders of magnitude higher than for the corresponding reaction of (*N*-X),*N*-methylethylamine under similar conditions. In both cases the decomposition rate of the (*N*-Br)-alcoholamine is *ca.* one order of magnitude faster than for the analogous (*N*-Cl)-derivative. Taking this into account, and considering the fact that the change of inductive effect due

Table 2. Second order rate constants observed for the base-promoted decomposition of different (*N*-X)-amines and (*N*-X)-alcoholamines. I = 1.0 M. Unless stated T = 298.15 K.

Compound	$k_{HO^-}\cdot10^4$ / mol^{-1}·dm^3·s^{-1}	$k_{TFE}\cdot10^4$ / mol^{-1}·dm^3·s^{-1} [a]	$k_{HFPr}\cdot10^4$ / mol^{-1}·dm^3·s^{-1} [a]
(*N*-Cl),*N*-methylethanolamine	402 ± 4[b]		
”	681 ± 5	152 ± 9	0.50 ± 0.03
”	1205 ± 18[c]		
”	1904 ± 19[d]		
(*N*-Br),*N*-methylethanolamine	2447 ± 47		
(*N*-Cl),*N*-methylethylamine	1.88 ± 0.07		
(*N*-Br),*N*-methylethylamine	42.2 ± 0.4		
(*N*-Cl),*N*-ethylethanolamine	8200[e]		
(*N*-Cl),*N*-diethylamine	2.03[e]		

[a] TFE = 2,2,2-trifluoroethoxide ion; HFPr = 1,1,1,3,3,3-hexafluoro-2-propoxide ion, [b] 293.15 K, [c] 303.15 K, [d] 308.15 K, [e] Ref. 10

to the replacement of $-CH_3$ by $-CH_2OH$ at one of the reaction centers of the molecule (σ^* ($-CH_2OH$) = 0.56, σ^* ($-CH_3$) = 0.00)[25] would not explain a rate enhancement of two orders of magnitude, it follows that the decomposition through Zaitsev elimination must be minimal. A parallelism can be established with the base-promoted decomposition of aliphatic secondary (*N*-X)-amines,[26] so that the contribution of Hoffmann elimination should be also negligible. Thus, the intramolecular elimination and fragmentation pathways depicted in Scheme 1 remain to be considered.

The reaction mechanism shown in Scheme 2 has been proposed for the base-promoted decomposition of (*N*-Cl),*N*-ethylethanolamine, involving a fast ionization of the -OH group that leads to the corresponding alkoxide, which may decompose through two different pathways.[10]

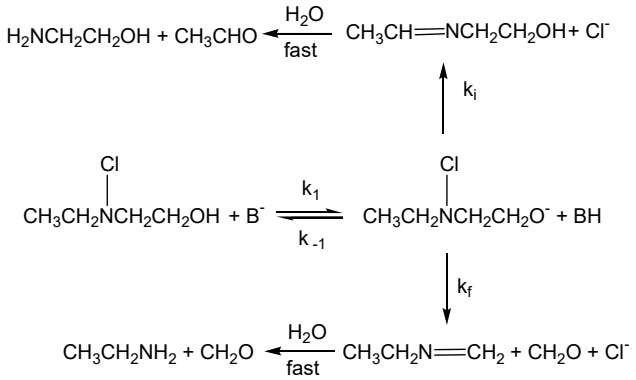

Scheme 2. Mechanism proposed for the base-promoted decomposition of (*N*-Cl),*N*-ethylethanolamine.[10]

Product analyses allow determination of the relative weight, and hence rate constants, of each of the two pathways. The reaction products expected for the base-promoted decomposition of (*N*-X),*N*-methylethanolamine through each of the pathways depicted in Scheme 1 are summarised in Table 3.

Table 3. Reaction products expected for the base-promoted decomposition of one mole of (*N*-X),*N*-methylethanolamine when the reaction takes place through the pathways shown in Scheme 1.

Hoffmann elimination	Zaitsev elimination	Intramolecular elimination	Fragmentation
CH_2O	$HOCH_2CHO$	CH_2O	2 CH_2O
$NH_2CH_2CH_2OH$	CH_3NH_2	$NH_2CH_2CH_2OH$	CH_3NH_2
X^-	X^-	X^-	X^-

Since methylamine and ethanolamine were obtained in similar concentrations (Table 1), both intramolecular elimination and fragmentation pathways must take place concurrently and contribute to the rate.

The yields of formaldehyde obtained (Table 1) can only be understood in terms of the fragmentation pathway being relevant in the overall decomposition mechanism: one mole of the starting (*N*-X),*N*-methylethanolamine leads to two moles of formaldehyde. Consequently, the two main paths in the decomposition of (*N*-X),*N*-methylethanolamine are intramolecular elimination and fragmentation. The corresponding contribution of each one, estimated from product analysis is collected in Table 4.

Assuming the fast acid-base preequilibrium (K_1) shown in Scheme 2 is displaced towards reactants, due to the high basicity of the alkoxide[10], the corresponding rate equation is:

$$r = k \cdot K_1 \cdot ([B^-]/[BH]) \cdot [(N\text{-X}),N\text{-methylethanolamine}] \quad (3)$$

where $k = k_f + k_i$. Taking into account the acidity constants of the base ($K_{a(BH)}$) and of the hydroxyl group of the alcoholamine ($K_{a(-OH)}$), and considering that $K_1 = K_{a(BH)}/K_{a(-OH)}$, equation 3 becomes:

Table 4. Estimated contributions of intramolecular elimination and base-assisted fragmentation to the base-promoted decomposition of (*N*-X),*N*-alkylethanolamines.

System	%Frag.	%Intramol.
(*N*-Cl),*N*-methylethanolamine + HO^-	67	33
(*N*-Br),*N*-methylethanolamine + HO^-	55	45
(*N*-Cl),*N*-methylethanolamine + $CF_3CH_2O^-$	67	33
(*N*-Cl),*N*-methylethanolamine + $(CF_3)_2CHO^-$	33	67
(*N*-Cl),*N*-ethylethanolamine + HO^-	14[a]	86[a]

[a] Ref. 10

$$r = (k \cdot K_{a(-OH)}/K_w) \cdot [HO^-] \cdot [(N\text{-X}),N\text{-methylethanolamine}] \quad (4)$$

where K_w is the self-ionisation constant of water.

Thus, $k_{obs} = (k_f + k_i) \cdot K_{a(-OH)}/K_w) \cdot [OH^-]$, *i.e.*, the rate equation derived from the mechanism in Scheme 2 implies specific base catalysis, whereas general base catalysis is found here (eq. 2). Both pathways show second order rate constants that are dependent on base strength, as shown in Figure 2.

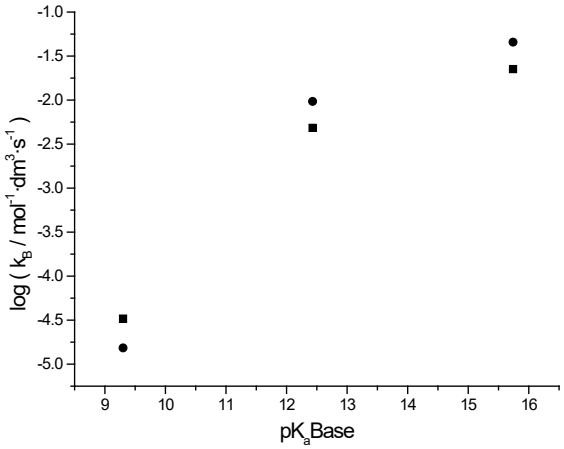

Figure 2. Dependence of the second order rate constant (k_B) on base strength for (*N*-Cl),*N*-methylethanolamine. (●) Fragmentation, (■) Intramolecular elimination.

Although product analyses are in agreement with the overall reaction scheme (Scheme 2), the fast ionisation preequilibrium at the –OH group is not appropriately accounted for by the current results, making necessary revisiting the mechanism of decomposition of (*N*-Cl),*N*-ethylethanolamine.

On the basis of the dependence of the second order rate constants with the pK_a of the base (Figure 2), a proton transfer from the -OH to the base could be suggested as the rate limiting step. However, the differences obtained in the rate of decomposition of (*N*-Br),*N*-methylethanolamine and (*N*-Cl),*N*-methylethanolamine rule out this possibility (Table 2). The dependence of the observed rate constants on the concentration of any base present in the medium together with the correlation between the second order rate constant and the pK_a of the base point to a base-assisted processes. In order to avoid an acid-base preequilibrium, the concerted process shown in Scheme 3 can be proposed as reaction mechanism. Since the hydrolysis of imines is fast, in the rest of this paper we refer to the initial stages, prior to imine hydrolysis. Thus, the corresponding rate law would be:

$$r = k \cdot [B^-] \cdot [(N\text{-X}),N\text{-methylethanolamine}] \quad (5)$$

where $k = k_f + k_i$ and $k_{obs} = k \cdot [B^-]$. Thus, the proton transfer from the -OH group would be dependent on base strength. The fact

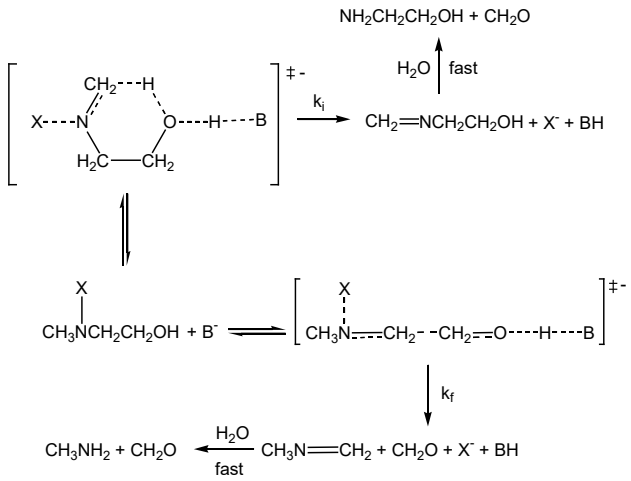

Scheme 3. Mechanism proposed for the base-assisted decomposition of (*N*-X),*N*-alkylethanolamines.

that Br^- is a better nucleofuge than Cl^- agrees with a concerted mechanism, explaining the higher rate of decomposition observed for (*N*-Br),*N*-methylethanolamine.

Transition states can be put forward for both pathways in which six bonds would be simultaneously involved, the most characteristic being a C=O bond formation and C-C bond breaking for the base-assisted fragmentation, and an H-O bond formation and C-H bond breaking for the intramolecular elimination. Although a simple estimation based on bond energies[27] suggests the intramolecular process (*ca*. -359 kJ) to be twice as exothermic as the base-assisted fragmentation (*ca*. -143 kJ), the product yields (Table 4) point to a similar $\Delta G^{\ddagger}$ for both processes. Additional information is supplied by the activation parameters, obtained from the study of the effect of temperature on the rate constants for the reaction between (*N*-Cl),*N*-methylethanolamine and HO^- (Table 5), and using the product distribution to resolve the two pathways.

Table 5. Experimental activation parameters obtained for the HO^--assisted decomposition of (*N*-Cl),*N*-methylethanolamine.

Base-assisted fragmentation	
$\Delta H^{\ddagger}$ / kJ·mol^{-1}	77 ± 2
$\Delta S^{\ddagger}$ / J·K^{-1}·mol^{-1}	-11 ± 6
$\Delta G^{\ddagger}$ (298.0 K)/ kJ·mol^{-1}	81 ± 2
Intramolecular elimination	
$\Delta H^{\ddagger}$ / kJ·mol^{-1}	74 ± 2
$\Delta S^{\ddagger}$ / J·K^{-1}·mol^{-1}	-29 ± 8
$\Delta G^{\ddagger}$ (298.0 K)/ kJ·mol^{-1}	82 ± 3

Due to the limited temperature range used for the determination of the activation parameters, and the fact that the experimental rate constants have been disected into the rate constants of the two parallel reactions on the basis of product distribution, the significance of the activation parameters should be taken with caution. The values obtained show that in fact $\Delta G^{\ddagger}$ is very similar for both processes, and agree with the proposed mechanism. Taking into account the bonds involved in the transition state, $\Delta H^{\ddagger}$ is expected to be rather similar for both processes, which is found. The $\Delta S^{\ddagger}$ values point to a more ordered transition state for the intramolecular elimination. This is reasonable, as achieving the cyclic disposition at the TS is more entropy demanding than reaching an open transition state. A value of $\Delta S^{\ddagger} \sim 0$ would be expected for the base-assisted fragmentation, its sign depending on the extent to which the bonds involved at the transition state are formed or broken, as well as on solvation changes.

A further step in the characterization of the transition states is the use of reaction maps[28,29]. Strictly speaking such bidimensional representations would only be appropriate to describe processes

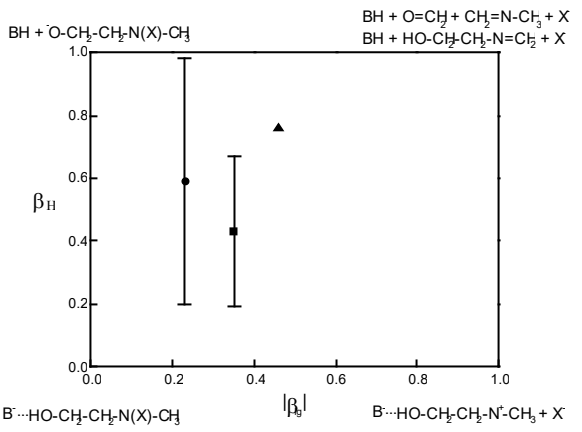

Figure 3. Reaction map for the processes under consideration. (■) Intramolecular elimination, experimental, (●) Base-assisted fragmentation, experimental, (▲) Base-assisted fragmentation, computational.

in which two major molecular events are involved, while in this case six bonds are breaking and forming cooperatively. Still, for a concerted process a plot of its progress in terms of proton transfer to the base and N-X bond breaking, should be a reasonable approximate approach. The estimation of the concertedness of the process and of the structure of the transition state can be done in terms of Brønsted's β_H, and of the Brønsted-like parameter β_{lg}, *i.e.*, the slopes of the plot of log (k_B / M^{-1}·s^{-1}) *vs* pK_a (BH) and log (k_X / M^{-1}·s^{-1}) *vs* pK_a (XH), respectively. The linearity of such plots is understood as evidence for the reaction with different bases and / or leaving groups having rather similar transition states. The synchroneity of the concerted process can be estimated as $|\beta_H - |\beta_{lg}||$, a value of 0 being obtained for a synchronous process and 1 for an uncoupled stepwise reaction.

Due to the nature of the reaction under study, only two points are available to make a crude estimation of the degree of N-X bond breaking (β_{lg}). On the other hand, the Brønsted plot is not linear for either pathway, as evident from Figure 2, which implies a variable degree of proton transfer to the base depending on its strength. The weaker the base the steeper the slope, *i.e.*, the degree of proton transfer is higher as the pK_a of the base decreases. Keeping this in mind and assuming that a linearization of the log (k_B / M^{-1}·s^{-1}) *vs* pK_a (BH) plot is an oversimplification, both TS's can be located on a reaction map (Figure 3).[28,29] It must be noted here that the free energy surfaces are different for the two processes, *i.e.*: the species on the upper right corner are not the same for each pathway. However, as the proton transfer and the N-X bond breaking are the processes under consideration, plotting them together allows comparison of the location of transition states. The error bars shown represent the change in the slopes in the Brønsted plot (Figure 2) as the strength of the base decreases: from 0.20 to 0.98 for the base-assisted fragmentation and from 0.19 to 0.67 for the intramolecular elimination.

Accordingly, as the points lie outside the axes, both pathways can be described as concerted, the degree of synchroneity depending on the base strength. Both processes are almost synchronous with stronger bases, the hydrogen abstraction from the -OH group being slightly ahead of the N-X bond breaking. As the base weakens, the imbalance[30] increases and the degree of proton transfer changes, being well ahead of the N-X bond breaking. In this case fragmentation is highly asynchronous. When $(CF_3)_2CHO^-$ is involved, the proton is almost fully transferred, whereas the N-X bond is only 25% broken. Such facts are in agreement with the change on the yield of reaction products on going from HO^- to $(CF_3)_2CHO^-$ (Table 4).

From the $\Delta G^{\ddagger}$ values for the decomposition of (*N*-Br),*N*-methylethanolamine, it could be interpreted that the change from N-Cl to the weaker N-Br bond accelerates both the base-assisted fragmentation process by lowering $\Delta G^{\ddagger}$ *ca.* 3 kJ·mol^{-1} and the

intramolecular elimination pathway by decreasing $\Delta G^{\ddagger}$ *ca.* 4 kJ·mol^{-1}. The fact that the intramolecular elementary process is favoured supports the proposed mechanism; this pathway should be more sensitive to changes in the nucleofuge.

Table 4 reflects a dramatic change in the relative contribution of the two pathways for the HO$^-$-assisted decomposition of (*N*-Cl),*N*-ethylethanolamine, the intramolecular elimination being the most favorable pathway in that case. Such a difference can be easily explained in terms of the increased acidity of the hydrogen being transferred and the enhanced stability of the N-C double bond being formed due to the presence of the methyl group on the C transferring the hydrogen, which lowers the intramolecular elimination energy barrier. Considering again the effect of this change on $\Delta G^{\ddagger}$, the fragmentation pathway shows a $\Delta G^{\ddagger}$ that is lower by *ca.* 2 kJ·mol^{-1} than that of (*N*-Cl),*N*-methylethanolamine, rather similar to the effect observed when changing –Cl to –Br on the N. The effect observed on the intramolecular elimination is a reduction of *ca.* 8-9 kJ·mol^{-1} in $\Delta G^{\ddagger}$, in agreement with the previous statements.

Electronic structure calculations of the *in vacuo* HO$^-$-assisted fragmentation of (*N*-Cl),*N*-methylethanolamine led to the same mechanism proposed on an experimental basis, *i.e.*, a two-step mechanism (Scheme 3) in which the first step corresponds to the fragmentation and the second to the hydrolysis of the *N*-methylmethanimine intermediate, yielding a second molecule of formaldehyde and methylamine. The results obtained cannot be explained in terms of the three-step mechanism, involving a Grob fragmentation as rate limiting step, proposed previously for the reaction between (*N*-Cl),*N*-ethylethanolamine and HO$^-$.[10] Attempts to find a stepwise mechanism *via* proton transfer followed by N-Cl cleavage were unsuccessful.

The -OH proton withdrawal is accompanied by a major internal reorganization taking place at the TS. It has been found that not only H-O and N-Cl bonds, but six bonds form and break concertedly. The theoretical TS for the rate limiting step is depicted in Figure 4.

A plot of the theoretically-determined progress of O-H and Cl-N bond breakages at the TS is shown on the reaction map of Figure 3. The difference can be attributted to the approximations underlying the experimental reaction maps, etc. For instance, to experimentally estimate β_H several bases are used, and thus the value reported for the degree of proton transfer is an average rather than a specific value for each base, the same being true for the nucleofuges. Conversely, the computationally obtained value is estimated for the reactants involved in the calculation, (*N*-Cl),*N*-methylethanolamine and HO$^-$. Another common experimental assumption is the conservation of bond order at the transition state. Computational results suggest this is not the case for this process. Figure 4 shows the Wiberg bond indexes[21] at the TS, and it follows that the sum of bond orders involved in the proton transfer is not one, and the pattern will not change on moving from the transition structure to the transition state.

Wiberg bond indexes[21] have been used to analyse the synchroneity of the base-assisted fragmentation, which can be estimated by means of the Sy parameter proposed by Moyano *et al.*[31] Sy = 1 meaning fully synchronous bond reorganization, while Sy = 0 implies a stepwise mechanism. Here, we find Sy = 0.77, *i.e.*: the HO$^-$-assisted fragmentation of (*N*-Cl),*N*-methylethanolamine is a slightly asynchronous process. This value can be compared to the experimental one, 0.95, estimated as $(1 - |\beta_H - |\beta_{lg}||)$. Having in mind the approximations underlying this value (*vide supra)* the agreement is acceptable.

Thermodynamic parameters for the fragmentation process were theoretically calculated considering RIC, transition structure and PIC as the relevant stationary points along the reaction coordinate. (Table 6)

As usual, theoretical and experimental activation values are different.[32] The experimental $\Delta S^{\ddagger}$ =-11±6 J·K^{-1}·mol^{-1}, a small negative value, does not clearly show the bimolecularity of the rate limiting step. Likewise, the theoretical value of $\Delta S^{\ddagger}$ =

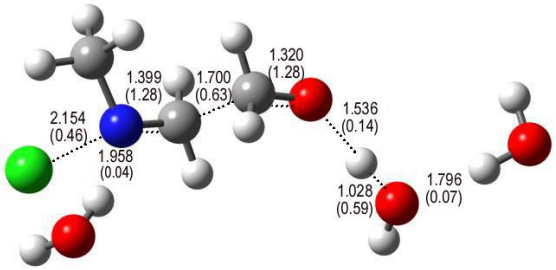

Figure 4. Theoretically obtained TS for the HO$^-$-assisted fragmentation of (*N*-Cl),*N*-methylethanolamine *in vacuo* obtained at the B3LYP/6-31++G** computational level. Dotted lines indicate bond-breaking / bond-forming processes. Distances between relevant atoms are shown and the corresponding Wiberg bond orders given between parenthesis.

1 J·K^{-1}·mol^{-1}, is close to zero but still the computational results clearly describe this process as bimolecular. Furthermore, these data are very similar to the value obtained for the intermolecular elimination of (*N*-Cl),*N*-methylethylamine, $\Delta S^{\ddagger}$ = -4±26 J·K^{-1}·mol^{-1}, which is also accepted as a bimolecular process.[11,26] The reaction proceeds from two reactant molecules, (*N*-Cl),*N*-methylethanolamine and HO$^-$, to products, four molecules: *N*-methylmethanimine, formaldehyde, Cl$^-$, and a discrete H_2O molecule. Thus, a noticeable increment of entropy is expected as the reaction progresses. The increase of ΔS from RIC to PIC has been theoretically calculated as 67 J·K^{-1}·mol^{-1}, therefore, the activation entropy for this process corresponds to a change from a two-molecule RIC into a TS which is a cluster of four partially bonded molecules. This explains the low absolute value obtained for $\Delta S^{\ddagger}$. It is a remarkable fact that the calculated value for the enthalpy change from RIC to PIC (-139 kJ·mol^{-1}) is in good agreement with the value of the reaction enthalpy change estimated from average bond enthalpies (-143 kJ·mol^{-1}).[27]

Table 6. B3LYP/6-31++G** thermodynamic parameters obtained for the HO$^-$-assisted fragmentation of (*N*-Cl),*N*-methylethanolamine.

RIC to TS	
$\Delta H^{\ddagger}$ / kJ·mol^{-1}	28
$\Delta S^{\ddagger}$ / J·K^{-1}·mol^{-1}	1
$\Delta G^{\ddagger}$ (298.0 K)/ kJ·mol^{-1}	27
RIC to PIC	
ΔH^0 / kJ·mol^{-1}	-139
ΔS^0 / J·K^{-1}·mol^{-1}	67
ΔG^0 (298.0 K)/ kJ·mol^{-1}	-159

Single point calculations on the previously optimized structures using the polarizable continuum model (PCM)[24] were carried out to include bulk solvation. The free energy of solvation values for RIC, TS and PIC are -215, -227 and -177 kJ·mol^{-1} respectively. The variation comes from the change in solvation on going from the HO$^-$ to Cl$^-$ as the reaction proceeds. The net effect of solvation using PCM is to reduce both the activation barrier and exergonicity of the reaction. Calculations with more sophisticated models to better match the experimental values are in progress.

More important than the coincidence of the thermodynamic computational and experimental values seems the fact that both experiment and calculation support a concerted asynchronous process, where the proton transfer from the -OH group to the HO$^-$ is ahead of the N-Cl bond cleavage.

Conclusions.

The presence of the -OH group in (*N*-X),*N*-methylethanolamine increases the rate of decomposition relative to the parent (*N*-X),*N*-methylethylamine to an extent that cannot be explained just in terms of inductive effect. The rate enhancement observed, as well as the analysis of the products generated, led us to the conclusion that only two pathways, an intramolecular elimination and a base-assisted bimolecular fragmentation, are involved.

Both routes take place *via* two consecutive steps. The first one in both cases is a bimolecular step involving the attack of the base to the hydroxylic hydrogen of the (*N*-X),*N*-methylethanolamine. In the elementary intramolecular elimination process such attack triggers the proton transfer from the methyl group to the hydroxylic oxygen and the departure of the halide. In the elementary base-assisted fragmentation, the proton transfer from the hydroxyl group forces the breakage of the molecule, formaldehyde acts as electrofuge group, the halide anion plays the nucleofuge role, and *N*-methylmethanimine is formed. Kinetic evidences suggest both the elementary base-assisted fragmentation and the intramolecular elimination take place through concerted asynchronous steps. The attack of the base on the hydroxylic hydrogen is ahead of the rest of the molecular events, the weaker the base the more asynchronous the process becomes. Subsequent fast hydrolysis of the intermediate imine formed through each route explains the percentages of products found. B3LYP/6-31++G** density functional calculations on the elementary base-assisted fragmentation step support the mechanism proposed.

Acknowledgements.

D.R. Ramos thanks the Spanish *Ministerio de Educación, Cultura y Deporte* for a PhD *F.P.U.* grant. This work was funded by the autonomous government *Xunta de Galicia* through project PGIDT99PX110302B. Thanks are also due to the *Centro de Supercomputación de Galicia (CESGA)* and the *Centro de Cálculo (UJI, Castelló)* for providing computing facilities through access to Fujitsu® VPP 300E and Silicon Graphics® Origin 2000 computers, respectively.

References.

† This work is part of DRR *PhD thesis*. * Correspondence regarding this manuscript should be sent to this author.

(1) Thomas, E. L.; Grisham, M. B.; Jefferson, M. M. *Methods in Enzymology* **1986**, *132*, 585.
(2) Klebanoff, S. J. *J. Bacteriol.* **1968**, *95*, 2131.
(3) Thomas, E. L.; Grisham, M. B.; Jefferson, M. M. *J. Clin. Invest.* **1983**, *72*, 441.
(4) Schraufstatter, I. U.; Browne, K.; Harris, A.; Hyslop, P. A.; Jackson, J. H.; Quehenberger, O.; Cochrane, C. G. *J. Clin. Invest.* **1990**, *85*, 554.
(5) Klebanoff, S. J. In *Inflammation: basic principles and clinical correlates*; Gallin, J. I., Snyderman, R., Eds.; Lippincott Williams & Wilkins: Philadelphia, 1999, p 721.
(6) Miller, S. *Environ. Sci. Technol.* **1993**, *27*, 2292.
(7) Henschler, D. *Angew. Chem. Int. Ed. Engl.* **1994**, *33*, 1920.
(8) Frazén, R.; Kronberg, L. *Environ. Sci. Technol.* **1994**, *28*, 2222.
(9) Budavari, S., Ed. *The Merck index : an encyclopedia of chemicals, drugs, and biologicals*; 12th ed. ed.; Whitehouse Station Merck & Co: Rahway, New Jersey, U.S.A., 1996.
(10) Armesto, X. L.; Canle L., M.; Carretero, P.; García, M. V.; Santaballa, J. A. *Tetrahedron* **1997**, *53*, 2565.
(11) Armesto, X. L.; Canle L., M.; García, M. V.; Santaballa, J. A. *Chem. Soc. Rev.* **1998**, *27*, 453.
(12) Hückel, W.; Hanack, M. *Angew. Chem. Int. Ed. Engl.* **1967**, *6*, 534.
(13) Grob, C. A.; Schiess, P. W. *Angew. Chem. Int. Ed. Engl.* **1967**, *6, No. 1.*, 1.
(14) Armesto, X. L.; Canle L., M.; Losada, M.; Santaballa, J. A. *Int. J. Chem. Kinet.* **1993**, *25*, 331.
(15) Page, M. I.; Webster, P. S. *J. Chem. Soc. Perkin Trans. 2* **1990**, 813.
(16) EPA Method 8315A,"Determination of carbonyl compounds by high performance liquid chromatography (HPLC)," 1996.
(17) Frisch, M. J.; Trucks, G. W.; Schlegel, H. B.; Scuseria, G. E.; Robb, M. A.; Cheeseman, J. R.; Zakrzewski, V. G.; Montgomery, J. A.; Stratmann, R. E.; Burant, J. C.; Dapprich, S.; Millam, J. M.; Daniels, A. D.; Kudin, K. N.; Strain, M. C.; Farkas, O.; Tomasi, J.; Barone, V.; Cossi, M.; Cammi, R.; Mennucci, B.; Pomelli, C.; Adamo, C.; Clifford, S.; Ochterski, J.; Petersson, G. A.; Ayala, P. Y.; Cui, Q.; Morokuma, K.; Malick, D. K.; Rabuck, A. D.; Raghavachari, K.; Foresman, J. B.; Cioslowski, J.; Ortiz, J. V.; Stefanov, B. B.; Liu, G.; Liashenko, A.; Piskorz, P.; Komaromi, I.; Gomperts, R.; Martin, R. L.; Fox, D. J.; Keith, T.; Al-Laham, M. A.; Peng, C. Y.; Nanayakkara, A.; Gonzalez, C.; Challacombe, M.; Gill, P. M. W.; Johnson, B. G.; Chen, W.; Wong, M. W.; Andres, J. L.; Head-Gordon, M.; Replogle, E. S.; Pople, J. A.; Revision A.7 ed.; Gaussian, Inc.: Pittsburgh PA, 1998.
(18) Becke, A. D. *J. Chem. Phys.* **1993**, *98*, 5648.
(19) Clark, T.; Chandrasekhar, J.; Spitznagel, G. W.; Schleyer, P. v. R. *J. Comput. Chem.* **1983**, *4*, 294.
(20) Lee, C.; Yang, W.; Parr, R. G. *Phys. Rev. B* **1988**, *37*, 785.
(21) Wiberg, K. B. *Tetrahedron* **1968**, *24*, 1083.
(22) Reed, A. E.; Weinstock, R. B.; Weinhold, F. J. *J. Chem. Phys.* **1985**, *83*, 735.
(23) Reed, A. E.; Weinstock, R. B.; Weinhold, F. J. *Chem. Rev.* **1988**, *88*, 899.
(24) Miertus, S.; Scrocco, E.; Tomasi, J. *J. Chem. Phys.* **1981**, *55*, 117.
(25) Hansch, C.; Leo, A. *Substituent Constants for Correlation Analysis in Chemistry and Biology*; Wiley Interscience: New York, 1979.
(26) Abia, L. *PhD thesis.* Universidade da Coruña. A Coruña, Spain, 1993.
(27) Lide, D. R., Ed. *CRC Handbook of chemistry and physics*; 83d ed.; ed. CRC Press, Inc.: Boca Ratón, 2002.
(28) Jencks, W. P. *Chem. Rev.* **1985**, *85*, 512.
(29) O'Ferrall, R. A. M. *J. Chem. Soc. (B)* **1970**, 274.
(30) Bernasconi, C. F. *Adv. Phys. Chem.* **1992**, *27*, 119.
(31) Moyano, A.; Pericàs, M. A.; Valentí, A. *J. Org. Chem.* **1989**, *54*, 573.
(32) Jensen, F. *Introduction to Computational Chemistry*; John Wiley & Sons: Chichester, 1999.